Australian Journal of Biomedical Research
(eISSN 3083-4708)

Original Article

Beetroot Fruit Powder Attenuates Cardiotoxicity Induced by Monosodium Glutamate via Inhibition of Oxidative Stress and Inflammation in Rats

Blessing Oluwapelumi Oyebamiji[1], Moshood Abiola Folawiyo[1,2], Blessing Tolulope Owolabi[1], Ayodeji Folorunsho Ajayi[3]

[1]*Department of Physiology, Faculty of Basic Medical Sciences, Ekiti State University, Ado-Ekiti, Ekiti State, Nigeria*
[2]*Department of Physiology, College of Medicine and Allied Health Sciences, Venite University, Iloro-Ekiti, Ekiti State, Nigeria*
[3]*Department of Physiology, Faculty of Basic Medical Sciences, Ladoke Akintola University of Technology, Ogbomoso, Nigeria*

Received: Sep 17, 2025
Accepted: Nov 27, 2025

Corresponding author's email: oyebamiji.b.2003003177@eksu.edu.ng

Abstract:

Background: Cardiotoxicity, defined as damage to cardiac muscle resulting from exposure to toxic substances, is a growing concern in both environmental and medical contexts. Monosodium glutamate (MSG), a widely used food additive, has been implicated in cardiac toxicity through mechanisms involving inflammation, oxidative stress, and apoptosis. Beetroot (Beta vulgaris), rich in nitrates, betalains, and flavonoids, possesses strong antioxidant and anti-inflammatory properties that may counteract MSG-induced cardiac damage.

Objective: This study investigated the cardioprotective potential of beetroot fruit powder (BFP) against MSG-induced cardiotoxicity in male Wistar rats by evaluating its effects on inflammatory, oxidative, apoptotic, cardiac functional markers, and DNA fragmentation index.

Methods: Fifty male Wistar rats (185–205 g) were randomly divided into five groups: control, MSG-only, MSG + low-dose BFP (0.18 g/kg), MSG + high-dose BFP (0.36 g/kg), and MSG recovery group. MSG was administered orally (6 g/kg) for 21 days. BFP treatments were co-administered with MSG. On day 22, cardiac tissues were harvested and analyzed for inflammatory markers (MPO, NO, CRP, TNF-α, IL-1β, NF-κB), oxidative stress markers (MDA, SOD, CAT, GSH, GPx, GST), cardiac enzymes (LDH, SDH, CK, GGT), caspase-3 activity, and DNA fragmentation (TUNEL assay). Histological examination was also performed.

Results: MSG exposure significantly elevated pro-inflammatory cytokines, oxidative stress, caspase-3 activity, and cardiac dysfunction markers, alongside pronounced DNA fragmentation and histological alterations. BFP co-treatment, particularly at the high dose, significantly attenuated these changes by reducing pro-inflammatory markers, restoring antioxidant enzyme levels, normalizing cardiac enzyme activities, and lowering DNA fragmentation index. Histology confirmed structural recovery of cardiac tissue in BFP-treated groups. These results underscore the potential of BFP as a dietary intervention to mitigate chemically induced myocardial injury. While the MSG dose used exceeds typical human exposure, this model provides valuable mechanistic insights. Future studies should explore chronic, lower-dose MSG exposure, gene-level regulatory mechanisms, and translational trials in humans.

Conclusion: Beetroot fruit powder demonstrates a potent cardioprotective effect against MSG-induced toxicity by modulating oxidative, inflammatory, apoptotic, and functional biomarkers. These findings highlight its potential as a natural therapeutic agent for mitigating chemically-induced cardiac injury.

Keywords: Beetroot Fruit Powder; Monosodium Glutamate; Cardiotoxicity; Oxidative Stress; Inflamation

Introduction

Cardiotoxicity, defined as damage to the heart muscle caused by exposure to hazardous substances, is a growing concern in both environmental and medical contexts. It frequently manifests as inflammation, oxidative stress, and apoptotic damage, resulting in structural remodeling and impaired cardiac function.1 Among the various chemicals implicated, dietary additives such as monosodium glutamate (MSG) have received increased scientific interest due to their potential participation in organ-specific and systemic toxicity, including adverse effects on the cardiovascular system.

MSG, although extensively used as a flavor enhancer and usually viewed as safe, has been documented to disturb redox equilibrium, raise pro-inflammatory cytokine levels, and impair mitochondrial function in various organs, including the heart.2 High-dose MSG exposure has been experimentally associated with increased production of nuclear factor kappa B (NF-κB), myeloperoxidase (MPO), nitric oxide (NO), tumor necrosis factor-alpha (TNF-α), interleukin-1 beta (IL-1β), and C-reactive protein (CRP), all of which contribute to inflammation-induced cardiac damage. Furthermore, endogenous antioxidants, including glutathione peroxidase (GPx), catalase (CAT), and superoxide dismutase (SOD), are usually decreased, whereas oxidative indicators like malondialdehyde (MDA) are usually increased.3 These abnormalities can cause DNA fragmentation, a sign of permanent cell damage, and trigger apoptotic pathways via caspase-3. Moreover, the release of enzymes like succinate dehydrogenase (SDH) and lactate dehydrogenase (LDH) is a sign of compromised heart function and integrity.4

Given the accumulating evidence of MSG-induced cardiotoxicity, it is critical to find effective, natural treatments that might prevent or mitigate these detrimental consequences. The broad-spectrum bioactivity of beetroot (Beta vulgaris), a functional food rich in phytochemicals such as betalains, dietary nitrates, flavonoids, and polyphenols, has drawn researchers' curiosity. According to Clifford et al,5 beetroot has been shown to reduce pro-inflammatory pathways, oxidative damage, and enhance nitric oxide bioavailability. It has been demonstrated to benefit cardiovascular health in models of metabolic syndrome, ischemia-reperfusion injury, and hypertension. Despite these positive properties, little is known regarding its potential protective role against chemically induced cardiotoxicity, particularly when MSG exposure is present. The purpose of this study is to assess the cardioprotective benefits of beetroot fruit powder in male Wistar rats who have been exposed to MSG. It specifically explores the extent to which beetroot reduces cardiac inflammation, oxidative stress, apoptosis, DNA fragmentation, and dysfunction using biochemical, molecular, and histopathological techniques. This study fills a vacuum in the present knowledge while also contributing to the growing field of natural therapies in toxicology and cardiovascular health management.

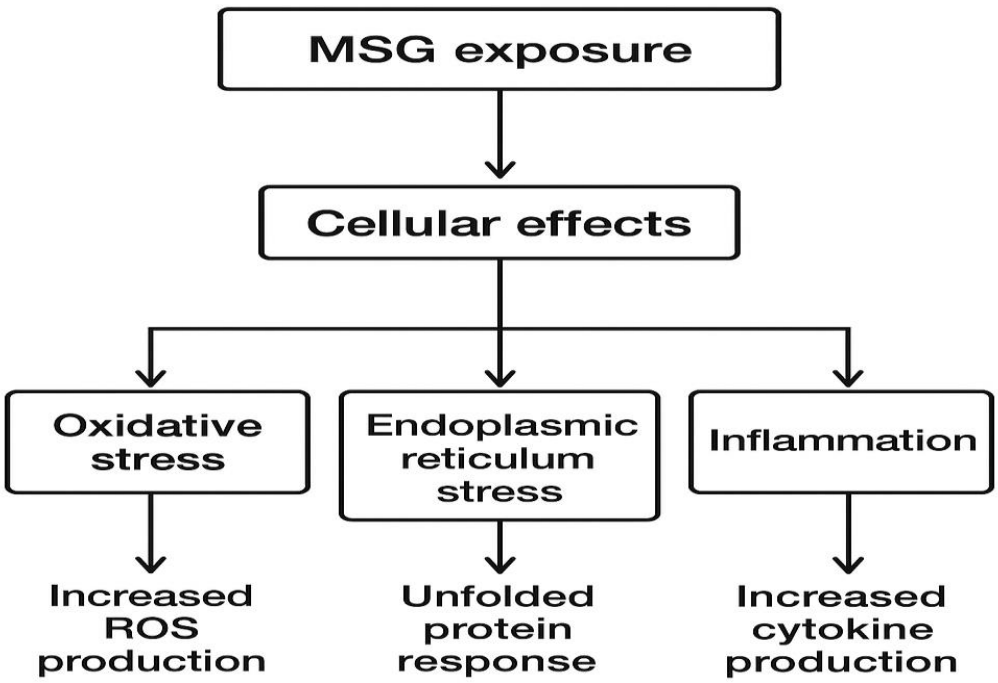

Materials

Chemicals and Drugs

All chemicals and drugs utilized in this study were of high-quality analytical grade. Beetroot Fruit Powder was purchased from Simply Precious Enterprise, Badagry, Lagos, Nigeria. Monosodium Glutamate (MSG) was purchased from Mich Mikedenson Nigeria Enterprises Limited, Ilorin, Nigeria. Ethanol, distilled water, and phosphate buffer were acquired from the Laboratory at the Physiology department at Ekiti State University (EKSU), Ado-Ekiti, Nigeria.

Animals

The study was carried out at the Central Animal house at EKSU. A total of fifty male Wistar rats weighing between 185 - 205kg were obtained from the same Central Animal House. The animals were kept under standard laboratory conditions and housed in well-aerated plastic cages with aluminium cover bedded with saw dust. They were fed with tap water and quality rat pellets (Tripods feed limited, Nigeria) on ad libitum. The research protocol approval was obtained from the Department of Physiology's Research Ethical Committee at Ekiti State University with the ethical number, EKSU/P100/2024/01/002.

Stock Solution Preparation

Throughout the study, MSG was administered at a dosage of 6 grams per kilogram (6 g/kg) (The stock solution was prepared by dissolving 0.6 grams of MSG in one milliliter (1 ml) of distilled water, with a concentration of 600 mg/ml.6 BFP was administered orally at two dosage levels: a low dose (0.18 g/kg body weight) and a high dose (0.36 g/kg body weight). The stock solutions were prepared by dissolving 0.18 g and 0.36 g of BFP in 1 mL of distilled water, resulting in concentrations of 180 mg/mL and 360 mg/mL, respectively. These doses were selected based on preliminary pilot testing and modified from dose ranges reported in previous studies investigating the physiological and therapeutic effects of beetroot powder in animal models. While literature reports vary widely in dosing, from 200 to 1000 mg/kg depending on the route, duration, and experimental model, the doses in this study were chosen to allow the evaluation of both sub-therapeutic and moderately therapeutic effects over a short-term exposure window. BFP was freshly prepared daily and administered via oral gavage for 21 consecutive days.7-8

Experimental Protocol

After acclimating the animals to the laboratory environment for fourteen days, the 50 male Wistar rats were randomly grouped into five groups of ten animals each (A, B, C, D, and E). Administration was done daily through oral routes for twenty-one days, and the animals were treated accordingly using oral cannulas as shown in Table I.

Table I: Experimental Grouping

Groups	Treatments	Dosage
Group 1	Negative control (distilled water)	1 ml/100 0kg body weight
Group 2	Positive control (MSG only)	0.6 g/100 g body weight
Group 3	MSG + BFP Low dose	0.18g/100g body weight
Group 4	MSG + BFP High dose	0.36g/100g bodyweight
Group 5	Recovery group	(MSG only and left for another 21 days after administration)

Sacrifice and Specimen/Tissue Collection

On day 22, 24 hours after the last dosage, the rats were weighed and culled with an intraperitoneal injection of ketamine-xyline (40mg/kg - 4mg/kg), as previously reported by Ajayi and Akhigbe,9 the hearts were collected, weighed, and recorded as previously documented. Blood samples were collected from the heart and centrifuged at 3000/RMP for 15 minutes to separate the serum from the clot. A portion of the heart was homogenized with a laboratory mortar and pestle in freshly produced phosphate buffer solution (pH 7.4), and the homogenate was kept at 800°C for biochemical analysis. The remaining piece of the heart was preserved in a vial with 10% neutral buffer formalin for histological examination.10

Biochemical Evaluation

Myeloperoxidase (MPO) Activity

Cardiac MPO activity was assessed according to the modified protocol of Goiffon et al.11 Approximately 50 mg of heart tissue was homogenized in 50 mM potassium phosphate buffer (pH 6.0) containing 0.5% hexadecyltrimethylammonium bromide (HTAB). After sonication and freeze–thaw cycles, the homogenate was centrifuged at 15,000 × g for 15 minutes at 4°C. The supernatant was incubated with o-dianisidine dihydrochloride and H_2O_2, and absorbance was measured at 460 nm. MPO activity was expressed as units per milligram of protein.

Estimation of Nitric Oxide (NO)

Nitric oxide production was determined by measuring its stable metabolite, nitrite, using the Griess reaction as described by Vargas-Maya et al.12 Tissue homogenates were deproteinized and incubated with equal volumes of 1% sulfanilamide and 0.1% N-(1-naphthyl)ethylenediamine in 2.5% phosphoric acid. The absorbance of the pink azo dye was read at 540 nm. Nitrite concentrations were calculated using a sodium nitrite standard curve.

C-Reactive Protein (CRP) Analysis

CRP levels in cardiac tissue homogenates were quantified using a high-sensitivity ELISA kit (Rat CRP ELISA Kit, e.g., Elabscience), following the manufacturer's instructions. Homogenates were added to ELISA plate wells pre-coated with anti-rat CRP antibodies. After incubation, substrate solution was added, and absorbance was measured at 450 nm. Concentrations were derived from the standard curve.

Determination of Tumor Necrosis Factor-alpha (TNF-α)

The electrochemical bioassay using Affibody®, a non-immunoglobulin protein, effectively detects TNF- levels in serum samples, with a detection limit of 38 pg/mL and a quantification range of 76-5000 pg/mL.13

Determination of Interleukin-1 Beta (IL-1β)

IL-1β concentration in cardiac tissue was quantified using a rat IL-1β ELISA kit as per the manufacturer's instructions. Standards and samples were incubated in antibody-coated wells, followed by detection antibodies and substrate development. Absorbance was measured at 450 nm.

Nuclear Factor kappa B (NF-κB) Activity

NF-κB p65 levels were evaluated using a rat-specific NF-κB ELISA kit. Cardiac tissue homogenates were prepared according to the kit protocol. After sequential incubation with detection antibodies and HRP conjugates, absorbance was recorded at 450 nm.

Malondialdehyde (MDA) Analysis

MDA, a marker of lipid peroxidation, was measured using the thiobarbituric acid reactive substances (TBARS) method, as adapted from Tsikas.14 Briefly, cardiac homogenates were mixed with thiobarbituric acid (TBA) and acetic acid, heated at 95°C for 60 minutes, and then cooled. The pink chromogen formed was extracted in butanol and measured at 532 nm. MDA concentration was expressed as nmol/mg protein using a standard curve of 1,1,3,3-tetramethoxypropane.

Superoxide Dismutase (SOD) Activity

SOD activity was measured based on its ability to inhibit the auto-oxidation of pyrogallol, following the method as modified by Islam et al15 Tissue homogenates were incubated with Tris-HCl buffer (pH 8.2) and pyrogallol. The rate of auto-oxidation was monitored at 420 nm, and one unit of SOD activity was defined as the amount causing 50% inhibition.

Catalase (CAT) Activity

Catalase activity was determined using the method of Afsar et al.16 In brief, cardiac homogenates were added to a solution containing 30 mM hydrogen peroxide in phosphate buffer (pH 7.0). The decomposition of H_2O_2 was monitored at 240 nm for 60 seconds. Results were expressed as μmol of H_2O_2 decomposed/min/mg protein.

Estimation of Glutathione (GSH)

GSH was estimated using Ellman's reagent (5,5′-dithiobis-(2-nitrobenzoic acid), DTNB). Cardiac tissue was homogenized in 5% sulfosalicylic acid and centrifuged. Supernatants were reacted with DTNB, and the absorbance of the yellow chromophore was measured at 412 nm. GSH levels were expressed as μmol/g tissue.17

Estimation of Glutathione Peroxidase (GPx)

GPx activity was evaluated using the NADPH-coupled method as described by Schwarz et al.18 Cardiac homogenates were incubated with hydrogen peroxide, glutathione, glutathione reductase, and NADPH. The decrease in absorbance at 340 nm due to NADPH oxidation was monitored. Activity was expressed as U/mg protein.

Glutathione-S-Transferase (GST) Activity

GST activity was determined spectrophotometrically using 1-chloro-2,4-dinitrobenzene (CDNB) as the substrate. Cardiac homogenates were incubated with CDNB and reduced GSH, and the conjugation reaction was monitored at 340 nm. The procedure was based on the method adapted by Robin et al.19

Determination of Lactate Dehydrogenase (LDH)

LDH activity in cardiac tissue was measured using the method of Klein et al,20 based on the oxidation of NADH to NAD^+ during the conversion of pyruvate to lactate. Cardiac homogenates were incubated with a reaction mixture containing 100 mM sodium phosphate buffer (pH 7.4), 0.15 mM NADH, and 1.5 mM pyruvate. The decrease in absorbance was recorded at 340 nm for 3 minutes. LDH activity was expressed as units per milligram of protein.

Determination of Succinate Dehydrogenase (SDH)

SDH activity was determined by monitoring the reduction of 2,6-dichlorophenolindophenol (DCPIP) as described by Moreno et al.21 Heart tissue homogenates were incubated with a reaction mixture containing sodium succinate (20 mM), potassium

phosphate buffer (pH 7.4), and DCPIP (40 μM). The decrease in absorbance at 600 nm was recorded. SDH activity was expressed in μmol/min/mg protein.

Creatine Kinase (CK) Analysis

CK activity was evaluated using a commercial CK assay kit or buffer containing creatine phosphate and ADP. CK catalyzes the conversion of creatine phosphate and ADP to creatine and ATP, coupled with a colorimetric detection of NADH consumption via hexokinase and glucose-6-phosphate dehydrogenase reactions. Absorbance was measured at 340 nm, and results were expressed as U/L.

Gamma-glutamyl Transferase (GGT) Activity

As Jiang et al22 described, GGT activity was measured spectrophotometrically using γ-glutamyl-p-nitroanilide as a substrate and glycylglycine as an acceptor. The formation of p-nitroaniline was measured at 405 nm. Results were expressed as units per liter (U/L) of tissue homogenate.

Caspase-3 Activity Assay

Caspase-3 activity in cardiac tissue was measured using a colorimetric assay based on the cleavage of the chromogenic substrate Ac-DEVD-pNA, following the method of Wynne and Elmes.23 Briefly, cardiac homogenates were prepared in lysis buffer and incubated with the substrate at 37 °C for 2 hours. The release of p-nitroaniline (pNA) was quantified by measuring absorbance at 405 nm. Caspase-3 activity was expressed as units per mg of protein.

DNA Fragmentation Index (TUNEL Assay)

Cardiac DNA fragmentation was assessed using the TUNEL (Terminal deoxynucleotidyl transferase dUTP Nick-End Labeling) assay according to the protocol adapted by Sharma et al.24 Paraffin-embedded cardiac sections were deparaffinized, rehydrated, and treated with proteinase K. DNA strand breaks were labeled with fluorescein-conjugated dUTP in the presence of terminal deoxynucleotidyl transferase (TdT). TUNEL-positive nuclei were visualized using fluorescence microscopy, and DNA fragmentation index (DFI) was expressed as the percentage of TUNEL-positive cells per field.

Histopathological Analysis

The collected hearts were fixed in Bouin's solution, dehydrated using an increasing ethanol series, and finally cleaned with toluene. The heart was imbedded at ambient temperature, then blocked in paraffin wax and kept in a 60°C incubator overnight. Hematoxylin and eosin (H&E) staining was performed on 5 μm thick paraffin slices of the heart. The stained slides were inspected using a light microscope, and photomicrographs were obtained at 100x and 400x magnifications.25

Statistical Analysis

The data was analyzed using the GraphPad Prism software (version 9.0, GraphPad Software, Inc.). Data are presented as mean ± SD. For multiple group comparisons, one-way ANOVA was used, followed by the Tukey post hoc test. P-values <.05 were considered statistically significant.

Results

Effect of BFP on body weight and heart weight in MSG exposed rats

Table II depicted the results of the effect of BFP on IBW, FBW, BWC, and HW in MSG exposed rats. The IBW and FBW showed no significant ($p>0.05$) difference across all the groups. The BWC revealed a significant ($p<0.05$) decrease in group 2 rats and an increase in group 4 rats when compared with control rats, a significant ($p<0.05$) increase in BWC of rats in groups 3, 4, and 5 when compared with group 2 rats were also observed, a significant ($p<0.05$) increase in group 4 rats, and a decrease in group 5 rats BWC when compared with groups 3 and 4 rats, respectively. Meanwhile, the HW showed a significant ($p<0.05$) decrease in groups 2, 3, and 5 rats when compared with group 1 rats. Besides, the HW also expressed a significant ($p<0.05$) increase in groups 4 and 5 rats when compared with group 2 rats.

Table II: Effect of BFP on Body weight and heart weight in rats exposed to MSG

	Groups				
	Group 1 (Control)	**Group 2 (MSG-exposed)**	**Group 3 (MSG-exposed+LD BFP)**	**Group 4 (MSG-exposed+HD BFP)**	**Group 5 (MSG-exposed-R)**
IBW (g)	193.00 ± 10.58	199.7 ± 7.57	194.7 ± 5.13	188.7 ± 3.51	193.00 ± 3.61

FBW (g)	216.70 ± 11.93	210.30 ± 7.64	217.30 ± 6.43	217.00 ± 2.00	215.00 ± 4.583
BWC (g)	23.67 ± 1.53	10.67 ± 1.53^{a}	22.67 ± 1.53^{b}	28.33 ± 1.53^{abc}	22.00 ± 1.00^{bd}
HW (g)	1.27 ± 0.12	0.83 ± 0.06^{a}	0.97 ± 0.06^{a}	1.23 ± 0.06^{bc}	1.07 ± 0.06^{ab}

Values are mean ± SD of 3 replicates, where a P < 0.05 vs control, b P < 0.05 vs MSG-exposed, c P < 0.05 vs MSG-exposed+LD BFP, and d P < 0.05 vs MSG-exposed+HD BFP, and IBW, FBW, BWC, and HW were initial body weight, final body weight, body weight change, and heart weight, respectively.

Effect of BFP on Cardiac MPO, NO, and CRP in MSG exposed rats

The results of cardiac MPO, NO, and CRP were as expressed in Figure 1. The result of cardiac MPO (Figure 1A) showed a significant (p<0.05) increase in groups 2, 3, and 5 rats when compared with the control rats, a significant (p<0.05) decrease in groups 3, 4, and 5 rats when compared with the group 2 rats, and a significant (p<0.05) decrease in groups 4 and 5 rats when compared with group 3 rats. The result of cardiac NO (Figure 1B) revealed a significant (p<0.05) increase in groups 2 and 3 rats when compared with the control rats, a significant (p<0.05) decrease in groups 3, 4, and 5 rats when compared with the group 2 rats, a significant (p<0.05) decrease in group 4 rats when compared with group 3 rats, and a significant (p<0.05) increase in group 5 rats when compared with group 4 rats, while the result of cardiac CRP (Figure 1C) depicted a significant (p<0.05) increase in group 2 rats when compared with the control rats and a significant (p<0.05) decrease in groups 3, 4, and 5 rats when compared with the group 2 rats.

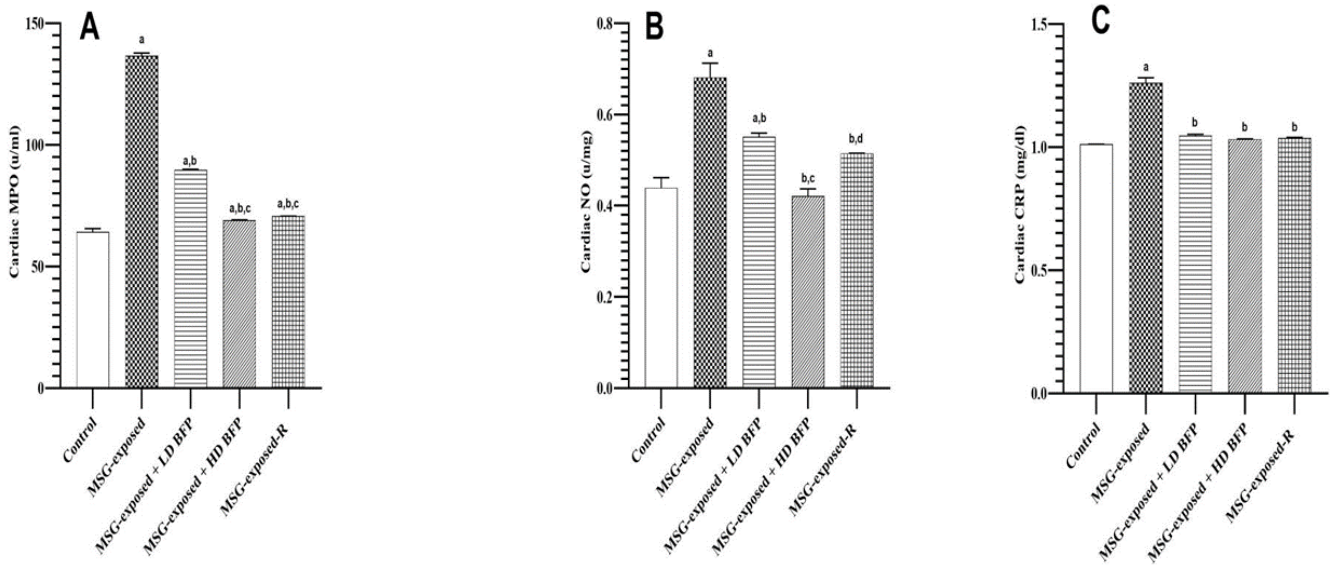

Fig I Effect of BFP on Cardiac MPO, NO, and CRP in MSG exposed rats. Values are mean ± SD of 3 replicates, where a P < 0.05 vs control, b P < 0.05 vs MSG-exposed, c P < 0.05 vs MSG-exposed+LD BFP, and d P < 0.05 vs MSG-exposed+HD BFP.

Effect of BFP on Cardiac IL-1β, TNF-α, and NF-kβ in MSG exposed rats

The results of cardiac IL-1β, TNF-α, and NF-kβ were as expressed in Figure 2. The result of cardiac IL-1β and TNF-α (Figure 2A and B) showed a significant (p<0.05) increase in groups 2, 3, 4, and 5 rats when compared with the control rats, a significant (p<0.05) decrease in groups 3, 4, and 5 rats when compared with the group 2 rats, a significant (p<0.05) decrease in groups 4 and 5 rats when compared with the group 3 rats, and a significant (p<0.05) decrease in group 5 rats when compared with the group 4 rats. The result of

cardiac NF-kβ (Figure 2C) revealed a significant ($p<0.05$) increase in group 2, 3, 4, and 5 rats when compared with the control rats, a significant ($p<0.05$) decrease in groups 3, 4, and 5 rats when compared with group 2 rats, and a significant ($p<0.05$) decrease in groups 4 and 5 rats when compared with the group 3 rats.

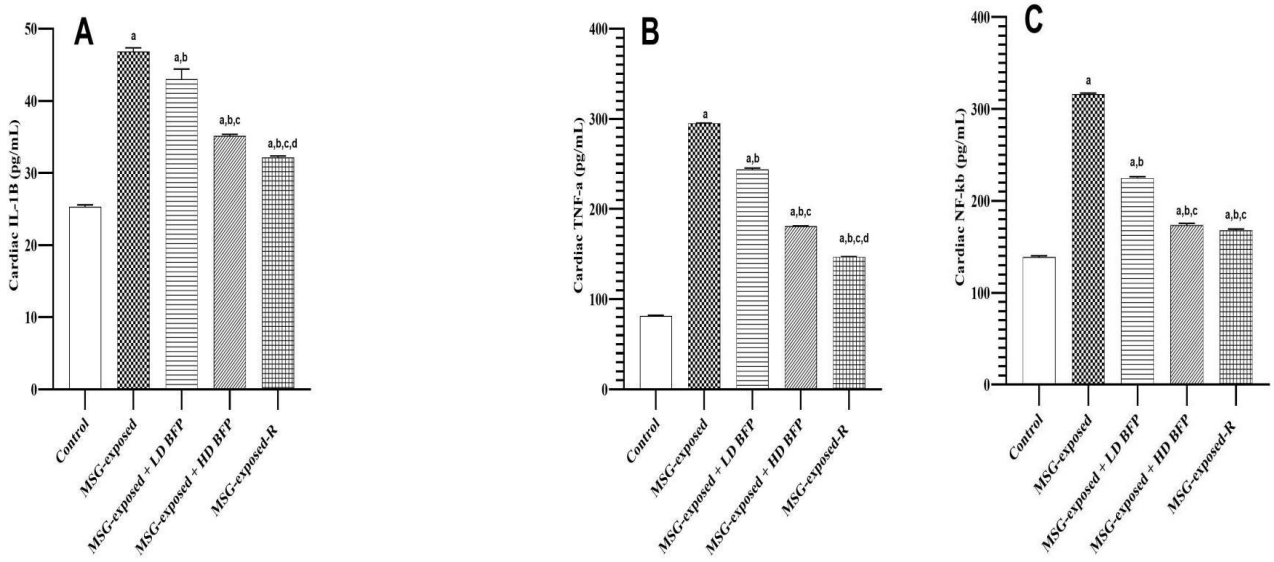

Figure 2: Effect of BFP on Cardiac IL-1β, TNF-α, and NF-kβ in MSG exposed rats.

Values are mean ± SD of 3 replicates, where a $P < 0.05$ vs control, b $P < 0.05$ vs MSG-exposed, c $P < 0.05$ vs MSG-exposed+LD BFP, and d $P < 0.05$ vs MSG-exposed+HD BFP.

Effect of BFP on Cardiac MDA, CAT, and SOD in MSG exposed rats

The results of cardiac MDA, CAT, and SOD were as expressed in Figure 3. The result of cardiac MDA (Figure 3A) showed a significant ($p<0.05$) increase in groups 2, 3, 4, and 5 rats when compared with the control rats, a significant ($p<0.05$) decrease in groups 3, 4, and 5 rats when compared with group 2 rats, and a significant ($p<0.05$) decrease in groups 4 and 5 rats when compared with group 3 rats. The result of cardiac CAT (Figure 3B) revealed a significant ($p<0.05$) decrease in groups 2, 3, 4, and 5 rats when compared with the control rats, a significant ($p<0.05$) increase in groups 3, 4, and 5 rats when compared with group 2 rats, and a significant ($p<0.05$) increase in groups 4 and 5 rats when compared with group 3 rats, while SOD (Figure 3C) result depicted a significant ($p<0.05$) decrease in groups 2, 3, 4, and 5 rats when compared with the control rats and a significant ($p<0.05$) increase in groups 4 and 5 rats when compared with groups 2 and 3 rats.

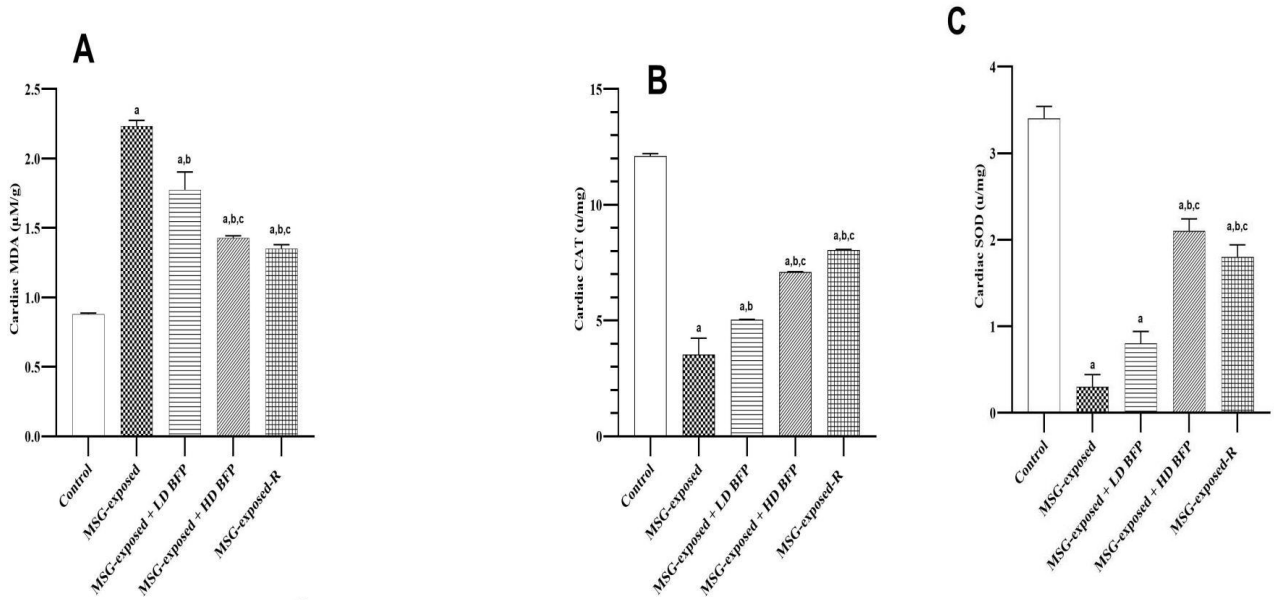

Figure 3: Effect of BFP on Cardiac MDA, CAT, and SOD in MSG exposed rats.

Values are mean ± SD of 3 replicates, where a P < 0.05 vs control, b P < 0.05 vs MSG-exposed, c P < 0.05 vs MSG-exposed+LD BFP, and d P < 0.05 vs MSG-exposed+HD BFP.

Effect of BFP on Cardiac GSH, GST, and GPx in MSG exposed rats

The results of cardiac GSH, GST, and GPx were as expressed in Figure 4. The result of cardiac GSH (Figure 4A) showed a significant (p<0.05) decrease in groups 2, 3, 4, and 5 rats when compared with the control rats, a significant (p<0.05) increase in groups 4 and 5 rats when compared with the group 2 rats, a significant (p<0.05) increase in group 4 rats when compared with the group 3 rats, and a significant (p<0.05) decrease in group 5 rats when compared with the group 4 rats. The result of cardiac GST (Figure 4B) revealed a significant (p<0.05) decrease in group 2, 3, 4, and 5 rats when compared with the control rats, and a significant (p<0.05) increase in groups 3, 4, and 5 rats when compared with the group 2 rats, while the result of cardiac GPx (Figure 4C) showed a significant (p<0.05) decrease in group 2, 3, 4, and 5 rats when compared with the control rats, a significant (p<0.05) increase in groups 3, 4, and 5 rats when compared with the group 2 rats, a significant (p<0.05) increase in groups 4 and 5 rats when compared with group 3 rats, and a significant (p<0.05) increase in group 5 rats when compared with the group 4 rats.

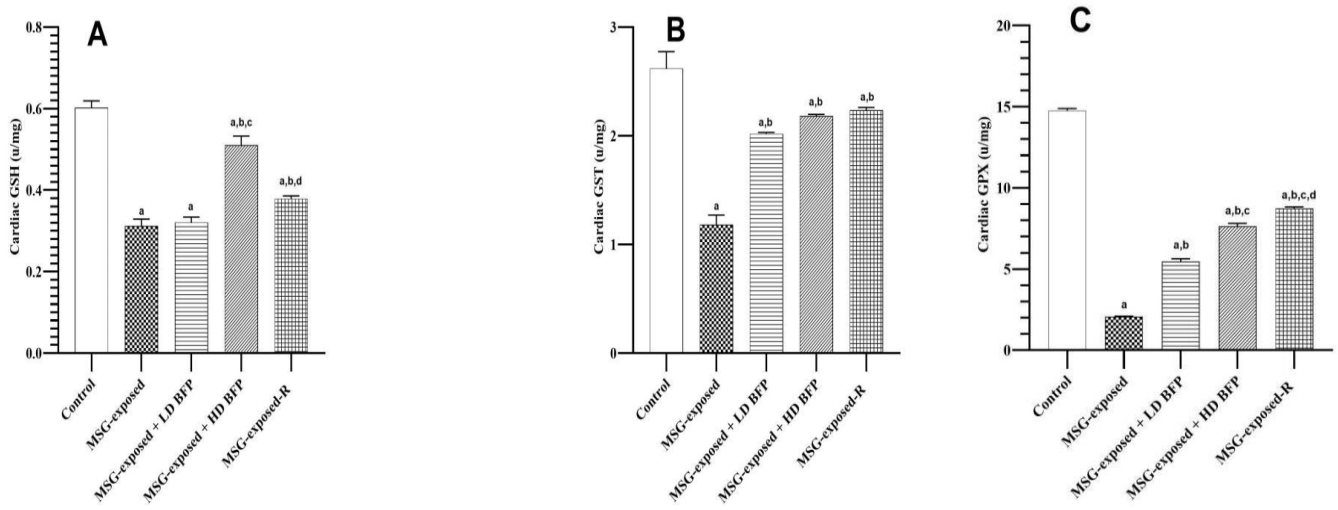

Figure 4: Effect of BFP on Cardiac GSH, GST, and GPx in MSG exposed rats.

Values are mean ± SD of 3 replicates, where a P < 0.05 vs control, b P < 0.05 vs MSG-exposed, c P < 0.05 vs MSG-exposed+LD BFP, and d P < 0.05 vs MSG-exposed+HD BFP.

Effect of BFP on Heart Functional markers in MSG exposed rats

The results of heart functions were as expressed in Figure 5. The result of SDH (Figure 5A) showed a significant (p<0.05) increase in groups 2, 3, 4, and 5 rats when compared with the control rats, a significant (p<0.05) decrease in groups 3, 4, and 5 rats when compared with group 2 rats, and a significant (p<0.05) increase in group 4 rats when compared with group 3 rats. The results of LDH and creatinine kinase (Figure 5B and D) showed a significant (p<0.05) increase in groups 2, 3, 4, and 5 rats when compared with the control rats, a significant (p<0.05) decrease in groups 3, 4, and 5 rats when compared with group 2 rats, and a significant (p<0.05) decrease in groups 4 and 5 rats when compared with group 3 rats. The result of GGT (Figure 5C) showed a significant (p<0.05) increase in groups 2, 3, 4, and 5 rats when compared with the control rats, a significant (p<0.05) decrease in groups 3, 4, and 5 rats when compared with group 2 rats, a significant (p<0.05) decrease in group 4 rats when compared with group 3 rats, and a significant (p<0.05) increase in group 5 rats when compared with group 4 rats.

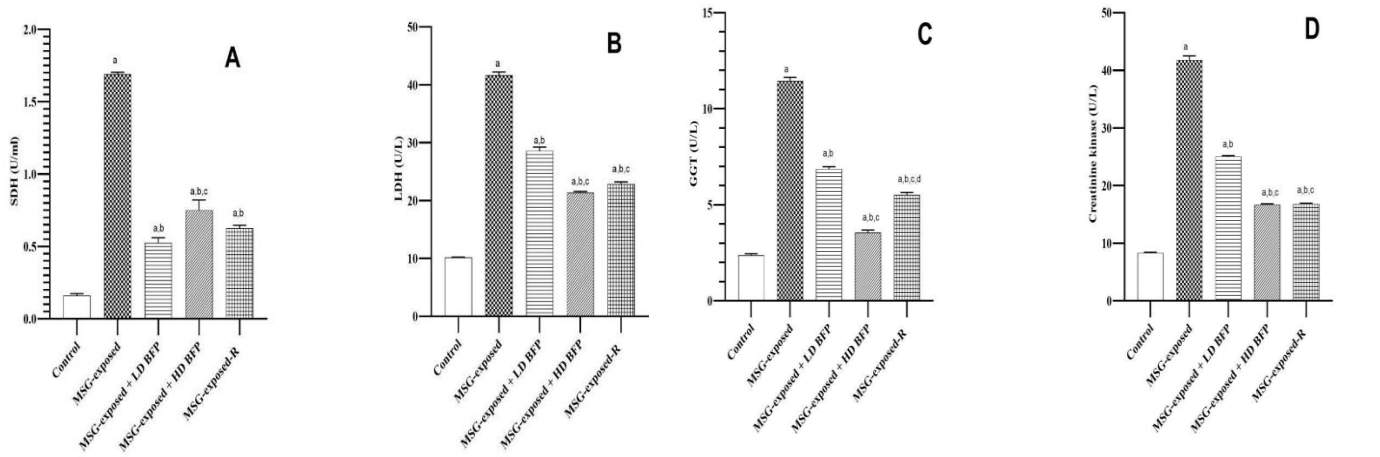

Figure 5: Effect of BFP on Heart Functional Markers in MSG exposed rats.

Values are mean ± SD of 3 replicates, where a P < 0.05 vs control, b P < 0.05 vs MSG-exposed, c P < 0.05 vs MSG-exposed+LD BFP, and d P < 0.05 vs MSG-exposed+HD BFP.

Effect of BFP on Heart Caspase-3 in MSG exposed rats

The results of heart caspase-3 was as expressed in Figure 6. The result of caspase-3 showed a significant (p<0.05) increase in groups 2, 3, and 5 rats when compared with the control rats, a significant (p<0.05) decrease in groups 3, 4, and 5 rats when compared with group 2 rats, and a significant (p<0.05) decrease in groups 4 and 5 rats when compared with group 3 rats.

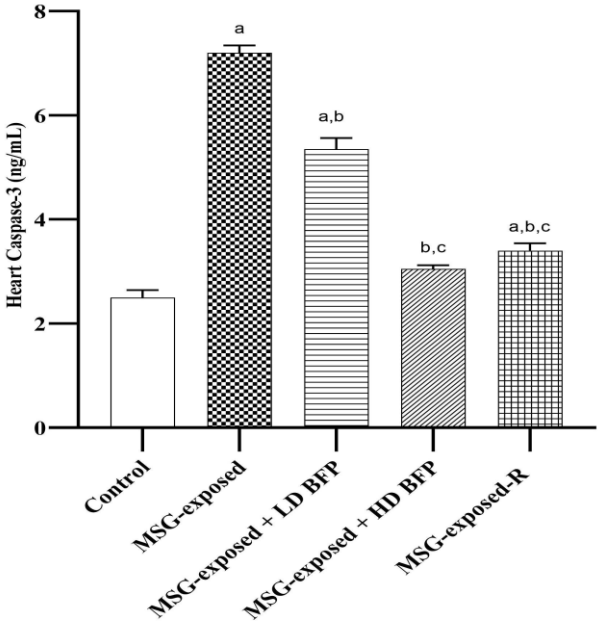

Figure 6: Effect of BFP on Heart caspase-3 in MSG exposed rats. Values are mean ± SD of 3 replicates, where a P < 0.05 vs control, b P < 0.05 vs MSG-exposed, c P < 0.05 vs MSG-exposed+LD BFP, and d P < 0.05 vs MSG-exposed+HD BFP.

Effect of BFP on Cardiac DFI in MSG Exposed Rats

The results of cardiac DFI was as expressed in Figure 7. The result of DFI revealed a significant (p<0.05) increase in groups 2, 3, and 5 rats when compared with the control rats, a significant (p<0.05) decrease in groups 3, 4, and 5 rats when compared with group 2 rats, a significant (p<0.05) decrease in groups 4 and 5 rats when compared with group 3 rats, and a

significant ($p<0.05$) increase in group 5 rats when compared with group 4 rats.

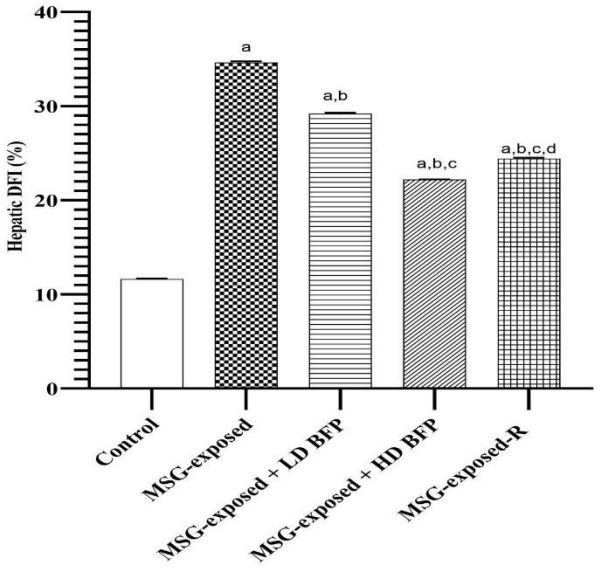

Figure 7: Effect of BFP on Cardiac DFI in MSG exposed rats.

Values are mean ± SD of 3 replicates, where a $P < 0.05$ vs control, b $P < 0.05$ vs MSG-exposed, c $P < 0.05$ vs MSG-exposed+LD BFP, and d $P < 0.05$ vs MSG-exposed+HD BFP.

Effect of BFP on Cardiac Histology in MSG exposed rats

Photomicrograph (Figure 8A) shows the heart tissue composed predominantly of the cardiac parenchyma and portal regions. The cardiac cells (C) appear polygonal and are disposed in sheet with a well outlined nucleus (N) the cardiac cells are separated by the sinusoids (S) with thin endothelial lining. The portal region (circle), composed of branches of the Cardiac portal vessels appear normal implying normal histomorphology of the heart tissue.

Photomicrograph (Figure 8B) shows the heart tissue composed predominantly of the cardiac parenchymal and portal regions. The cardiac cells (C) appear polygonal and are disposed in sheet with a well outlined nucleus (N). The cardiac cells are separated by the sinusoids (S) with thin endothelial). The portal region (circle), composed of branches of the Cardiac portal vessels (CPV), and showed vascular congestion (Star) and mild inflammatory cell infiltration (arrow head) implying inflammation of the heart tissue

Photomicrograph (Figure 8C) shows the heart tissue composed predominantly of the cardiac parenchymal and portal regions. The cardiac cells (C) appear polygonal and are disposed in sheet with a well outlined nucleus (N). The cardiac cells are separated by the sinusoids (S) with thin endothelial lining. The portal region (circle), composed of branches of the Cardiac portal vessels (CPV), and showed moderate inflammatory cell infiltration implying periportal inflammation of the heart tissue.

Photomicrograph (Figure 8D) shows the heart tissue composed predominantly of the cardiac parenchyma and portal regions. The cardiac cells (C) appear polygonal and are disposed in sheet with a well outlined nucleus (N) the cardiac cells are separated by the sinusoids (S) with thin endothelial lining. The portal region (circle), composed of branches of the cardiac portal vessels appear normal implying normal histomorphology of the heart tissue.

Photomicrograph (Figure 8E) shows the heart tissue composed predominantly of the cardiac parenchymal and portal regions. The cardiac cells (C) appear polygonal and are disposed in sheet with a well outlined nucleus (N). The cardiac cells are separated by the sinusoids (S) with thin endothelial lining. The portal region (circle), composed of branches of the cardiac portal vessels (CPV), and showed mild inflammatory cell infiltration (arrow head) implying cardiac cellular reaction to injury.

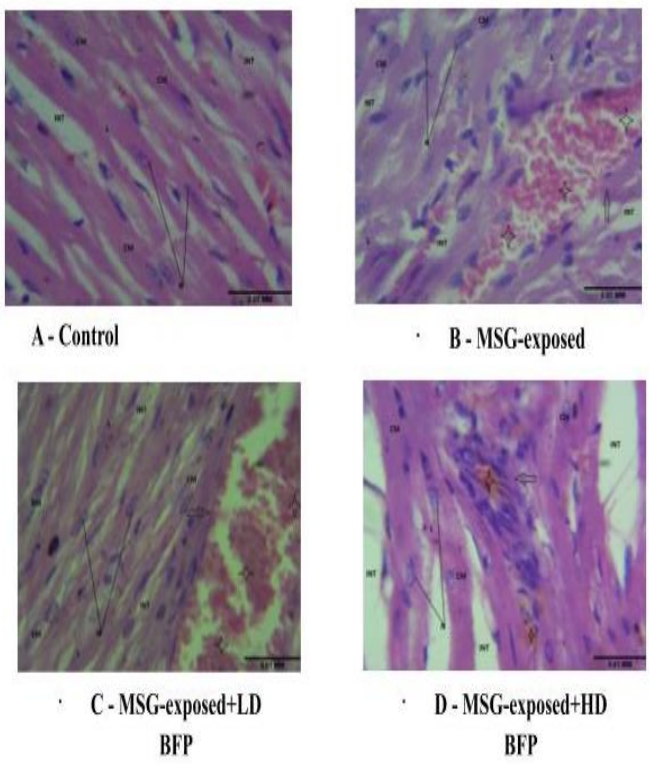

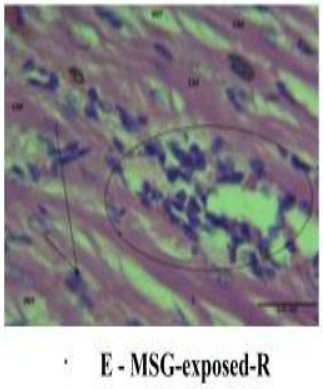

Figure 8: Photomicrograph of cardiac sections stained by H & E (Mg x400).

Where CM = cardiac muscles; L = Lateral branch; N = Nucleus; INT = Interstitiun

Discussion

BFP, a functional food rich in phytochemicals such betalains, flavonoids, and dietary nitrates, has received a lot of interest for its cardioprotective properties. In this work, BFP significantly reduced the biochemical, molecular, and histological changes caused by monosodium glutamate (MSG), a food toxicant that causes systemic oxidative and inflammatory stress. The observed effects indicate that BFP exerts its cardioprotective impact by influencing critical cellular pathways involved in oxidative stress, inflammation, apoptosis, and DNA damage, protecting cardiac structure and function.

The cardiotoxic effects of MSG were confirmed through the significant elevation of pro-inflammatory markers including MPO, NO, CRP, IL-1β, TNF-α, and NF-κB in MSG-exposed rats compared with controls. These cytokines and signaling mediators are key orchestrators of inflammatory responses that initiate and sustain myocardial injury.26 Persistent activation of NF-κB promotes the transcription of several pro-inflammatory genes, amplifying cardiac damage. The significant reduction of these markers following BFP administration, especially at higher doses, indicates that BFP mitigates inflammation by inhibiting NF-κB–dependent transcription and scavenging reactive free radicals through its polyphenolic and betalain content. These findings align with previous studies that demonstrated the anti-inflammatory potential of Beta vulgaris through suppression of NF-κB signaling and cytokine release.5,27

Oxidative stress also played a central role in MSG-induced cardiotoxicity, as evidenced by elevated malondialdehyde (MDA) levels and decreased antioxidant enzyme activities (SOD, CAT, GSH, GPx, and GST). This pattern indicates excessive reactive oxygen species (ROS) generation, lipid peroxidation, and impaired antioxidant defense systems, consistent with earlier findings on MSG-mediated cardiac injury.2 The substantial reduction in MDA levels and restoration of antioxidant enzyme activities in BFP-treated rats suggest potent redox regulatory effects of beetroot bioactives. These effects are likely mediated through activation of the Nrf2 signaling pathway, which upregulates endogenous antioxidant enzymes and enhances cellular resilience to oxidative damage.15,27

Similarly, assessment of cardiac function markers (LDH, SDH, CK, and GGT) revealed pronounced elevations in MSG-treated animals, confirming myocardial cell membrane disruption and enzymatic leakage. Treatment with BFP significantly reduced these enzyme levels, particularly at higher doses, suggesting stabilization of cardiomyocyte membranes and improved mitochondrial integrity. This protective response corroborates previous evidence that natural antioxidants can prevent enzyme leakage and limit necrotic cell death in cardiotoxicity models.28

Apoptosis, a key downstream effect of oxidative and inflammatory stress, was evident in the

elevated caspase-3 activity observed in MSG-exposed rats. The marked reduction of caspase-3 activity following BFP administration demonstrates the compound's anti-apoptotic potential, possibly achieved through inhibition of mitochondrial cytochrome-c release and suppression of pro-apoptotic signaling cascades. This anti-apoptotic mechanism aligns with beetroot's known ability to modulate intrinsic cell death pathways via its high nitrate and flavonoid content.5,29

In rats exposed to MSG, the DNA fragmentation index (DFI), a measure of genotoxic damage, also increased noticeably. Treatment with BFP decreased DNA fragmentation, which may indicate improved genomic stability and less oxidative DNA damage. The capacity of beetroot phytochemicals to assist DNA repair processes and neutralize reactive species that cause strand breaks may be the cause of this action.30

Histopathological examination further validated the biochemical results. Myocardial sections from MSG-exposed rats showed severe inflammatory infiltration, vascular congestion, and disorganized myofibrillar architecture—hallmarks of structural damage. Conversely, BFP-treated groups exhibited restored histoarchitecture with reduced inflammatory cell infiltration and preserved nuclei. These findings reinforce the biochemical and molecular evidence of recovery and demonstrate that BFP effectively reverses MSG-induced cardiac remodeling and dysfunction, similar to reports in other models of chemically induced cardiotoxicity.31

Collectively, these findings establish that beetroot fruit powder confers comprehensive cardioprotection against MSG-induced injury through integrated antioxidant, anti-inflammatory, and anti-apoptotic mechanisms. Its rich phytochemical composition and ability to restore redox balance suggest potential for its use as a natural therapeutic agent in preventing chemically induced cardiovascular disorders

Conclusion

These findings highlight the potential of beetroot fruit powder as a cardioprotective agent capable of averting chemically induced myocardial damage by suppressing inflammatory and apoptotic signaling, reducing oxidative stress, and stabilizing cardiac biomarkers. Its phytochemical makeup most likely contributes significantly to these effects, indicating its potential as a natural dietary intervention in the prevention or treatment of cardiac toxicity.

Acknowledgement

Author Contributions: Conceptualization, Folawiyo, M.A methodology Folawiyo, M.A and Oyebamiji, B.O.; validation, Folawiyo, M.A., Oyebamiji, B.O and Ajayi, A..; formal analysis, Oyebamiji, B.O Owolabi, B.T.; investigation, Folawiyo, Oyebamiji, B.O and Owolabi, B.T.; resources, Folawiyo, M.A data curation, Folawiyo, M.A.; writing – original draft preparation, Oyebamiji, B.O and Folawiyo, M.A.; writing – review and editing, Folawiyo, M.A, Oyebamiji, B.O, Ajayi, A. and Owolabi, B.T.; visualization, Folawiyo, M.A supervision, Folawiyo, M.A., Ajayi, A. project administration Folawiyo, M.A; Funding acquisition – Not applicable
All authors have read and agreed to the published version of the manuscript.

Acknowledgements: The Authors wish to acknowledge the support of the staff of the Department of Physiology Laboratory, Ekiti State University, Ado-Ekiti, Ekiti State, Nigeria.

Funding: The authors declare that no funds, grants, or other support were received during the preparation of this manuscript.

References

1. Mamoshina P, Rodríguez B, Bueno-Orovio A. Toward a broader view of mechanisms of drug cardiotoxicity. Cell Rep Med. 2021;2:100216. doi:10.1016/j.xcrm.2021.100216.
2. Hazzaa S, El-Roghy E, Eldaim M, Elgarawany G. Monosodium glutamate induces cardiac toxicity via oxidative stress, fibrosis, and P53 proapoptotic protein expression in rats. Environ Sci Pollut Res Int. 2020;27(16):20014-24. doi:10.1007/s11356-020-08436-6.
3. Ogunmokunwa A, Ibitoye B. Monosodium glutamate (MSG) exposure induced oxidative stress and disrupted testicular hormonal regulation, exacerbating reproductive dysfunction in male WISTAR rats. Endocr Metab Sci. 2025;:100226. doi:10.1016/j.endmts.2025.100226.
4. Dai C, Li Q, May H, Li C, Zhang G, Sharma G, et al. Lactate Dehydrogenase A Governs Cardiac Hypertrophic Growth in Response to Hemodynamic Stress. Cell Rep.

2020;32(8):108087. doi:10.1016/j.celrep.2020.108087.
5. Clifford T, Howatson G, West D, Stevenson E. The Potential Benefits of Red Beetroot Supplementation in Health and Disease. Nutrients. 2015;7(4):2801-22. doi:10.3390/nu7042801.
6. Nalugo H, Ninsiima HI, Kasozi KI, Nabirumbi R, Osuwat LO, Matama K, et al. Monosodium Glutamate Maintains Antioxidant Balance in the Neuro-Retinal Axis of Male Wistar Rats. J Exp Pharmacol. 2021;13:681-90. doi: https://doi.org/10.21203/rs.3.rs-508301/v1.
7. Abd-El-Fattah ME, Dessouki AA, Abdelnaeim NS, Emam BM. Protective effect of Beta vulgaris roots supplementation on anemic phenylhydrazine-intoxicated rats. Environ Sci Pollut Res Int. 2021;28(46):65731-42. doi:10.1007/s11356-021-15302-6.
8. Sarfaraz S, Ikram R, Munawwar R, Osama M, Gul S, Sufian M. Rising trend of Nutraceuticals: Evaluation of lyophilized beetroot powder at different doses for its hypolipidemic effects. Pak J Pharm Sci. 2021;34(4):1315-22. PMID: 34799303.
9. Ajayi AF, Akhigbe RE. Staging of the estrous cycle and induction of estrus in experimental rodents: an update. Fertil Res Pract. 2020;6:5. doi:10.1186/s40738-020-00074-3.
10. Zaidi AS, Muzaffar M, Gautam S, Alam I. Effect of curcumin on inflammatory and oxidative stress markers in Lipopolysaccharide induced animal models of pre-eclampsia. Physiology. 2024 May 1;39(S1):1737. doi:10.1152/physiol.2024.39.S1.1737.
11. Goiffon RJ, Martinez SC, Piwnica-Worms D. A rapid bioluminescence assay for measuring myeloperoxidase activity in human plasma. Nat Commun. 2015;6:6271. doi:10.1038/ncomms7271.
12. Vargas-Maya NI, Padilla-Vaca F, Romero-González OE, Rosales-Castillo EAS, Rangel-Serrano Á, Arias-Negrete S, et al. Refinement of the Griess method for measuring nitrite in biological samples. J Microbiol Methods. 2021;187:106260. doi:10.1016/j.mimet.2021.106260.
13. Baydemir G, Bettazzi F, Palchetti I, Voccia D. Strategies for the development of an electrochemical bioassay for TNF-alpha detection by using a non-immunoglobulin bioreceptor. Talanta. 2016;151:141-7. doi:10.1016/j.talanta.2016.01.021.
14. Tsikas D. Assessment of lipid peroxidation by measuring malondialdehyde (MDA) and relatives in biological samples: Analytical and biological challenges. Anal Biochem. 2017;524:13-30. doi:10.1016/j.ab.2016.10.021.
15. Islam MN, Rauf A, Fahad FI, Emran TB, Mitra S, Olatunde A, et al. Superoxide dismutase: an updated review on its health benefits and industrial applications. Crit Rev Food Sci Nutr. 2022;62(26):7282-300. doi:10.1080/10408398.2021.1913400.
16. Afsar T, Razak S, Batoo KM, Khan MR. Acacia hydaspica R. Parker prevents doxorubicin-induced cardiac injury by attenuation of oxidative stress and structural Cardiomyocyte alterations in rats. BMC Complement Altern Med. 2017;17(1):554. https://doi.org/10.1186/s12906-017-2061-0.
17. Kalinovic S, Stamm P, Oelze M, Daub S, Kröller-Schön S, Kvandová M, et al. Comparison of three methods for in vivo quantification of glutathione in tissues of hypertensive rats. Free Radic Res. 2021;55(9-10):1048-61. doi:10.1080/10715762.2021.2016735.
18. Schwarz M, Löser A, Cheng Q, Wichmann-Costaganna M, Schädel P, Werz O, et al. Side-by-side comparison of recombinant human glutathione peroxidases identifies overlapping substrate specificities for soluble hydroperoxides. Redox Biol. 2023;59:102593. doi:10.1016/j.redox.2022.102593.
19. Robin SKD, Ansari M, Uppugunduri CRS. Spectrophotometric Screening for Potential Inhibitors of Cytosolic Glutathione S-Transferases. J Vis Exp. 2020;(164). doi:10.3791/61924.
20. Klein R, Nagy O, Tóthová C, Chovanová F. Clinical and Diagnostic Significance of Lactate Dehydrogenase and Its Isoenzymes in Animals. Vet Med Int. 2020;2020:5346483. doi:10.1155/2020/5346483.
21. Moreno C, Santos RM, Burns R, Zhang WC. Succinate dehydrogenase and ribonucleic acid networks in cancer and other diseases.

Cancers (Basel). 2020;12(11):3237. doi:10.3390/cancers12113237.
22. Jiang L, Guo D, Wang L, Chang S, Li J, Zhan D, et al. Sensitive and selective SERS probe for detecting the activity of γ-glutamyl transpeptidase in serum. Anal Chim Acta. 2020;1099:119-25. doi:10.1016/j.aca.2019.11.041.
23. Wynne C, Elmes R. Utilising a 1,8-naphthalimide probe for the ratiometric fluorescent visualisation of caspase-3. Front Chem. 2024;12:1418378. doi:10.3389/fchem.2024.1418378.
24. Sharma R, Ahmad G, Esteves SC, Agarwal A. Terminal deoxynucleotidyl transferase dUTP nick end labeling (TUNEL) assay using bench top flow cytometer for evaluation of sperm DNA fragmentation in fertility laboratories: protocol, reference values, and quality control. J Assist Reprod Genet. 2016;33(2):291-300. doi:10.1007/s10815-015-0635-7.
25. Sridharan D, Pracha N, Dougherty JA, Akhtar A, Alvi SB, Khan M. A one-stop protocol to assess myocardial fibrosis in frozen and paraffin sections. Methods Protoc. 2022;5(1):13. doi:10.3390/mps5010013.
26. Reina-Couto M, Pereira-Terra P, Quelhas-Santos J, Silva-Pereira C, Albino-Teixeira A, Sousa T. Inflammation in human heart failure: major mediators and therapeutic targets. Front Physiol. 2021;12:746494. doi:10.3389/fphys.2021.746494.
27. Brzezińska-Rojek J, Sagatovych S, Malinowska P, Gadaj K, Prokopowicz M, Grembecka M. Antioxidant capacity, nitrite and nitrate content in beetroot-based dietary supplements. Foods. 2023;12(5):1017. doi:10.3390/foods12051017.
28. Bodor GS. Biochemical markers of myocardial damage. EJIFCC. 2016;27(2):95-111. PMID: 27683527.
29. Tan ML, Hamid SBS. Beetroot as a potential functional food for cancer chemoprevention, a narrative review. J Cancer Prev. 2021;26(1):1-17. doi:10.15430/JCP.2021.26.1.1.
30. Barnes JL, Zubair M, John K, Poirier MC, Martin FL. Carcinogens and DNA damage. Biochem Soc Trans. 2018;46(5):1213-24. doi:10.1042/BST20180519.
31. Banerjee A, Mukherjee S, Maji BK. Monosodium glutamate causes hepato-cardiac derangement in male rats. Hum Exp Toxicol. 2021;40(12_suppl):S359-S369. doi:10.1177/09603271211049550.